

BEHAVIOR AND RESPONSE OF AUTO-ADAPTIVE SEISMIC ISOLATION

Henri P. Gavin

Department of Civil and Environmental Engineering, Duke University
Durham, North Carolina, 27708–0287, USA (*henri.gavin@duke.edu*)

Unal Aldemir

I.T.U. Insaat Fakultesi, Mekanik Anabilim Dali
Maslak, 80626 Istanbul, TURKEY (*aldemiru@itu.edu.tr*)

Abstract

This paper describes auto-adaptive seismic isolation systems in terms of their behavior and their response to earthquake loads. The behavior of three types of auto-adaptive isolation systems are compared to a viscously-damped passive isolation system in terms of frequency response functions and shock spectra. By considering both generalized and historical earthquake excitation, this paper attempts to answer three questions: What are the drawbacks of high levels of passive viscous damping in seismic isolation; can these deficiencies be addressed in an auto-adaptive isolation system and simple feedback control algorithms, and, what is the best possible behavior one may expect from an auto-adaptive isolation system, within the dynamic constraints of the structural system and the auto-adaptive device? The first question is addressed using methods of linear structural dynamics, the second question makes use of the mathematical homogeneity of certain types of auto-adaptive systems, and the last question requires numerical and iterative solutions to the Euler-Lagrange equations.

Introduction

The use of seismic isolation bearings for the earthquake-protection of structures has increased from less than ten structures in 1985 to nearly forty structures in 2000 (Kelly 1997, EERC 1997). Detailed evaluation of structures subjected to the 1994 Northridge earthquake substantiate the effectiveness of this approach (Nagarajaiah and Xiahong, *et al.*, 2000). Indeed, the principle of detuning a structure from the dominant frequencies of strong ground motion while absorbing energy through damping in the isolation system works particularly well when long-period components are insignificant in the ground motion (Skinner *et al.*, 1993). The response of seismically isolated structures to long-period ground motion with strong velocity pulses has motivated the use of high damping in seismic isolation, to suppress the isolation deformation at the fundamental mode of the structure (Heaton *et al.* 1995, Kelly 1999).

The 1999 Chi-Chi Taiwan earthquake (M 7.3) resulted in 2,400 fatalities, 10,000 injuries, an infrastructure cost of \$8B, and a total economic loss exceeding \$30B (EERI, 1999a). The losses to Taiwan’s semi-conductor industry totaled \$1B, 95% of which was due solely to the disruption of business. In the US, computer memory prices quadrupled due to interruption of production in Taiwan (Sherin and Bartoletti, 1999).

Recently an Internet service exchange facility was installed in a seismically renovated warehouse in San Francisco (Lee, 2001). The seismic retrofit included strengthening of the existing structure and the installation of 96 friction pendulum isolation bearings with a 38 centimeter displacement capacity. The seismic retrofit was designed on the basis of a probabilistic seismic hazard analysis and an earthquake with a 950 year return period.

While heavy damping in the isolation system certainly reduces isolation deformation, in many cases it can also increase super-structure accelerations and deformations. Because the serviceability requirements for many critical facilities (including hospitals, emergency response centers, micro-fabrication centers, and especially data centers) are stringent with respect to acceleration levels, the decision to add heavy damping to isolation systems should consider the potential for the damping to increase super-structure accelerations and deformations.

This paper addresses this issue as a principle motivation for controllable, semi-active, or auto-adaptive damping in seismic isolation. In auto-adaptive seismic isolation systems, passive isolation bearings are combined with devices with controllable damping and an algorithm which controls the properties of these devices based on measurable quantities of the structural response of the system. In this study we make a distinction between structural behavior and structural response. To help uncover the deficiencies of passive damping in seismic isolation we study behavior via frequency response functions and shock spectra for idealized structures and compare those spectra to the behavior that is achievable via a simple controlled damping method and the “*best*” behavior achievable via a controlled damping approach. Ultimately structural response to diverse earthquake accelograms must be considered and we again compare passive viscous damping to controlled damping approaches.

Homogeneity of Behavior

Because the physical characteristics of auto-adaptive isolation systems are time-varying, Laplace-domain methods may not be applied (in general) to the analysis and design of the control system. This difficulty requires that the semi-active seismic isolation systems be evaluated via time-history analyses, which are typically carried out using one or more historical earthquake accelograms. For semi-active devices that do not exhibit force saturation effects, the response of semi-active isolation system scales linearly with the base excitation. This homogeneity property can be shown as follows: Consider the equations of motion of a MDOF structure excited by ground accelerations, \ddot{z} , and controlled by a controllable visco-elastic device with force, p .

$$M\ddot{r}(t) + C\dot{r}(t) + Kr(t) + bp(t) = -Mh\ddot{z}. \quad (1)$$

The device force follows

$$\dot{p} = -\frac{k}{c(v(t))}p(t) + kb^T\dot{r}(t) \quad (2)$$

where k is the device stiffness, $c(v(t))$ is the device's controllable damping rate, $c(v(t)) = c_{\min}(1 - v(t)) + c_{\max}v(t)$, and $v(t)$ controls the device following a simple feedback control algorithm (Karnopp *et al.*1974),

$$\dot{v} = -\frac{1}{T_v} \left[v(t) - H(p(t) \cdot b^T(h\dot{z}(t) + \dot{r}(t))) \right], \quad (3)$$

where T_v is the time-delay of the device and $H(\cdot)$ is the Heaviside step function, and $0 \leq v \leq 1$. These three equations contain the essential characteristics of an auto-adaptive isolation system. It can be seen that if the following substitutions are made, $\hat{z} = \alpha z$, $\hat{p} = \alpha p$, and $\hat{r} = \alpha r$, then \hat{z} , \hat{p} , and \hat{r} satisfy equations (1) — (3). Despite the fact that the Laplace transform of equation (3) can not be formed analytically, the response of this system scales linearly with the amplitude of the excitation. This fact enables the development and comparison of frequency response functions (through numerical time history simulations) without concern for the amplitude of the excitation.

Optimal Control

The optimal control policy for a nonlinear and non-autonomous system satisfies the Euler-Lagrange equations (Stengel 1994). Consider a general dynamical system

$$\dot{x}(t) = f(x(t), u(t); t), \quad x(0) = 0, \quad (4)$$

where the $x(t)$ is the n-dimensional state vector and $u(t)$ is the m-dimensional control vector. The objective of the control, $u(t)$ is to minimize an integral cost function,

$$J = \int_0^T \mathcal{L}(x(t), u(t); t) dt \quad (5)$$

subject to the constraints of the state equations (4). Necessary conditions for the optimality of $u(t)$ are given by the Euler-Lagrange equations.

$$\frac{\partial \mathcal{H}}{\partial u} = \frac{\partial f(x, u; t)}{\partial u} \lambda(t) + \frac{\partial \mathcal{L}(x, u; t)}{\partial u} = 0, \quad (6)$$

$$\dot{\lambda}(t) = -\frac{\partial f(x, u; t)}{\partial x} \lambda(t) - \frac{\partial \mathcal{L}(x, u; t)}{\partial x}, \quad \lambda(T) = 0, \quad (7)$$

where $\lambda(t)$ is the Lagrange multiplier or co-state vector and $\mathcal{H} = \mathcal{L} + \lambda(t)^T f$ is the Hamiltonian of the objective function. Equations (6) and (7) are solved iteratively, with each iteration improving up the optimality of the control time history, $u(t)$. In each iteration the gradient of the Hamiltonian is used as the search direction to improve $u(t)$.

$$u_{k+1}(t) = u_k(t) + K_k \frac{\partial \mathcal{H}(x, u; t)}{\partial u}, \quad (8)$$

where the update gain, K_k is determined at each global iteration to minimize u_{k+1} at the k^{th} iteration. It should be noted here that the co-state equation (7) must be integrated

backwards in time in order to satisfy the terminal condition $\lambda(T) = 0$. For this reason, truly optimal controls cannot be determined for non-autonomous systems in which the external disturbance is not known a-priori. Nonetheless, this method provides a very useful tool by which one may evaluate the performance or “optimality” of physically realizable control rules.

Numerical Examples

Numerical examples are carried out for a two degree of freedom seismically isolated structure. The mass of the isolation level is 100 tons and the mass of the super-structure is 300 tons. The isolation bearing system has a stiffness of 40 kN/cm and a damping of 2.5 kN/cm/s. The super structure has a stiffness of 79 kN/cm and a damping of 1.26 kN/cm/s. This structure has a 2.2 second fundamental period and a second mode with a 0.53 second period. The modal damping is 7% in the first mode and 16% in the second mode.

To examine the *behavior* of the structure, sinusoidal and pulse-like excitations are applied at different frequencies and pulse periods. The simulations are carried out until a harmonic steady state is reached (for the sinusoidal excitation) and until the peak response is attained for the pulse excitation. At each frequency of excitation, ω , the following transmissibility ratios are calculated:

$$T_{a1}(\omega) = \frac{|a_1(\omega)|}{|\ddot{z}(\omega)|} \quad (9)$$

$$T_{a2}(\omega) = \frac{|a_2(\omega)|}{|\ddot{z}(\omega)|} \quad (10)$$

$$T_{r1}(\omega) = \frac{|r_1(\omega)|}{|z(\omega)|} \quad (11)$$

$$T_{r2}(\omega) = \frac{|(r_2 - r_1)(\omega)|}{|z(\omega)|} \quad (12)$$

where $|a_1(\omega)|$ is the steady-state amplitude (for harmonic excitation) or the peak amplitude (for pulse excitation) of the absolute acceleration of the isolation level when the structure is excited at an angular frequency ω or a pulse period of $2\pi/\omega$. Similarly, a_2 is the absolute acceleration of the super-structure, r_1 is the drift of the isolation system, $r_2 - r_1$ is the inter-story drift of the super-structure, and $|\ddot{z}(\omega)|$ and $|z(\omega)|$ are the amplitudes of the ground acceleration and ground displacement at an angular frequency ω .

Transmissibility ratios are calculated for: (a) four levels of passive viscous damping in the isolation system (2.5, 5.0, 7.5 and 10.0 kN/cm/s corresponding to first mode damping ratios of 7%, 14%, 20%, and 27%); and (b) controllable viscous dampers with four levels of c_{\max} (2.5, 5.0, 7.5 and 10.0 kN/cm/s) and the control rule of equation (3). These transmissibility ratios are compared to the “optimal” behavior of auto-adaptive isolation systems with three types of controllable devices: a controllable viscous damper, a controllable stiffness device, and a controllable yielding (MR) device (Dyke *et al.*1996, Gavin *et al.*2001). The first two devices are modeled by equation (2) by choosing appropriate values for c and k . For the controllable damping device, k , c_{\min} and c_{\max} have values of 500kN/m, 1.0kN/cm/s and

7.5kN/cm/s, respectively. For the controllable stiffness device, k , c_{min} and c_{max} have values of 30kN/m, 0.1kN/cm/s and 650kN/cm/s, respectively. The MR device is modeled using an algebraic expression:

$$p = f_0 v \tanh(b^T r / d_0 + b^T \dot{r} / v_0) + k_0 b^T r + c_0 b^T \dot{r}, \quad (13)$$

where $f_0=100$ kN, $d_0=5$ cm, $v_0=4$ cm/s, $c_0=2$ kN/cm/s, and $k_0=3$ kN/cm. The cost function \mathcal{L} in the optimization is the absolute acceleration of the super-structure.

Results

Results are shown in figure 1. In parts 1(a) and 1(b), the passive damping cases are compared to three optimal control cases. Figure 1(a) corresponds to sinusoidal excitation while 1(b) corresponds to pulse excitation. The heavy line corresponds to first mode damping of 27% and the thin unbroken line corresponds to first mode damping of 7%. It is seen that the super-structure deformation and absolute acceleration, T_{r2} and T_{a2} increase with increased damping in the frequencies between the first and second natural frequencies ($1.1 < \omega/\omega_n < 3.1$) for sinusoidal excitation and at all frequencies above the first resonance for pulse-like excitation. These figures illustrate the answer to the first question: What are the drawbacks of high levels of passive viscous damping in seismic isolation? The goal of the auto-adaptive isolation system therefore is to suppress the response over the entire frequency range. The symbols (o, x, and *) correspond to the best performance achievable by the controllable viscous damper, the controllable yielding (MR) damper, and the controllable stiffness device. The objective is a reduction in the super structure accelerations, T_{a2} and all three devices achieve performance as good as, or better than, the passive damping system. The cost of reductions in T_{a2} are increases in the (un-penalized) base drift. This cost is especially clear in the case of the controllable stiffness device. Of particular interest is the fact that the controllable yielding (MR) device is able to reduce the super-structure accelerations without resulting in increased isolation drift. Also, note that in part (a) that the controllable stiffness device increases super-structure deformations by a factor of two at high frequencies as compared to passive damping systems, whereas in part (b) the controllable viscous device reduces the pulse-response of the super-structure deformation while increasing the isolation drift. In parts 1(c) and 1(d) the lines correspond to a controllable viscous damping device and the control rule 3. Unlike parts (a) and (b), in these two cases, we find that increasing the capacity of the damping device reduces all four transmissibilities over the entire frequency spectrum for both harmonic and pulse-like excitations. Furthermore, we find that the controllable viscous damping device using the control rule of equation (3) performs nearly as well as the “optimal” controller for all four transmissibility ratios.

Information regarding the *behavior* of auto-adaptive seismic isolation from the previous analysis guides the selection of a controllable yield force (MR) device for the earthquake *response* simulations. The device and structure are, again, equivalent to the system used in the frequency response studies. Four historical earthquakes are used in the analyses: the Sylmar and Rinaldi records of the 1994 Northridge earthquake, the JMA record of the 1995 Kobe earthquake and the El Centro record of the 1940 Imperial Valley earthquake. For each earthquake, time history analyses were run for five values of passive viscous damping in the

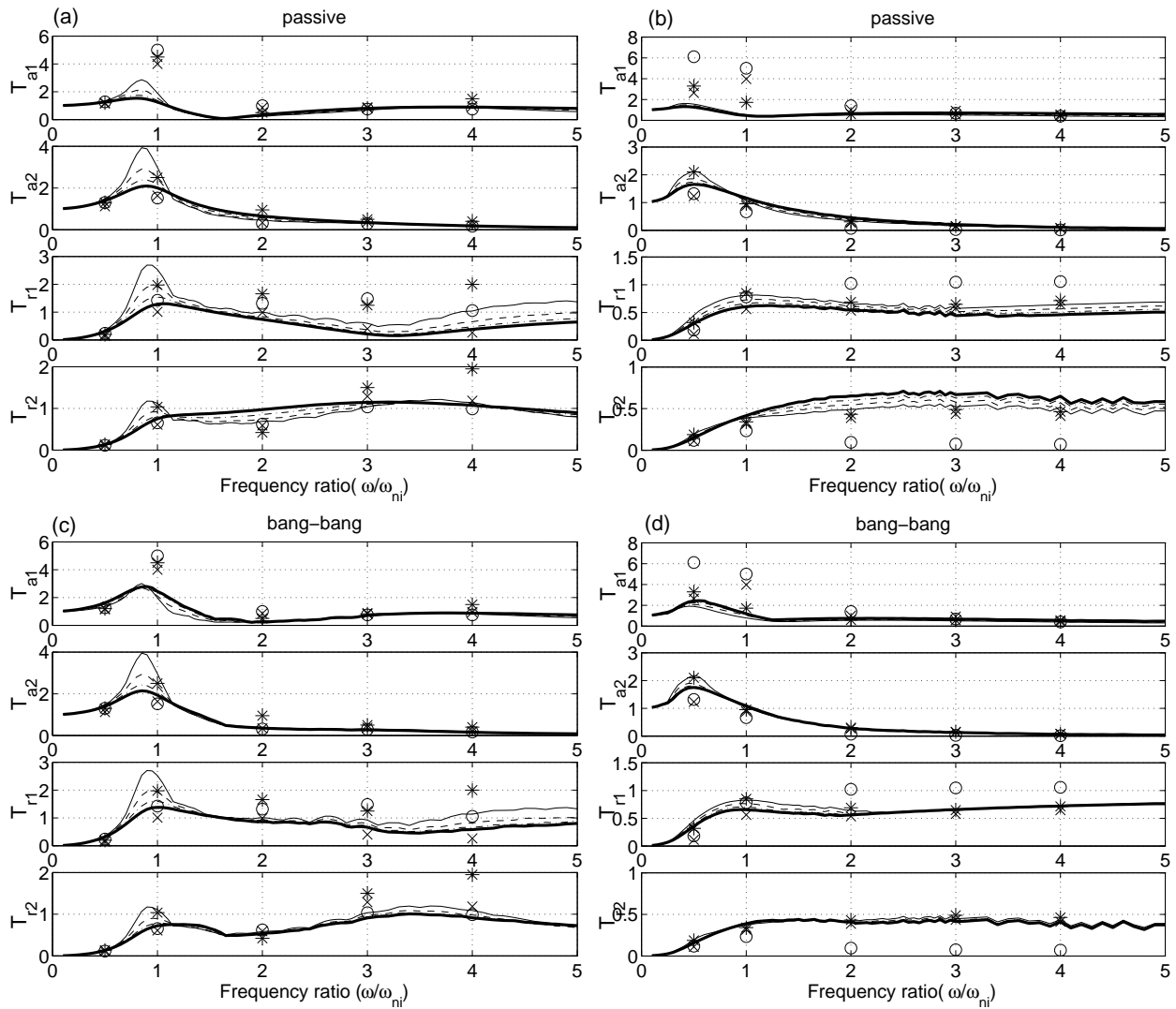


Figure 1: A comparison of passive damping and homogeneous auto-adaptive damping to optimal auto-adaptive damping.

isolation system, giving damping ratios from 7% to 27%. The peak super-structure acceleration, isolation drift, and inter-story drift are shown in figure 2 for these earthquakes as a function of the isolation damping. The level of damping which minimizes the acceleration and inter-story drift response (approximately $c = 5\text{kN/cm/s}$) is chosen as the best level of passive viscous damping. The response for this level of passive damping is compared to the “optimally” controlled isolation system and the auto-adaptive (MR) isolation (again using equation 3) in the accompanying bar charts. These bar charts illustrate that auto-adaptive control can reduce the super-structure acceleration and the super-structure deformation below any value achievable via passive viscous damping. Furthermore, this is achieved with isolation deformations that are comparable to very high levels of passive damping.

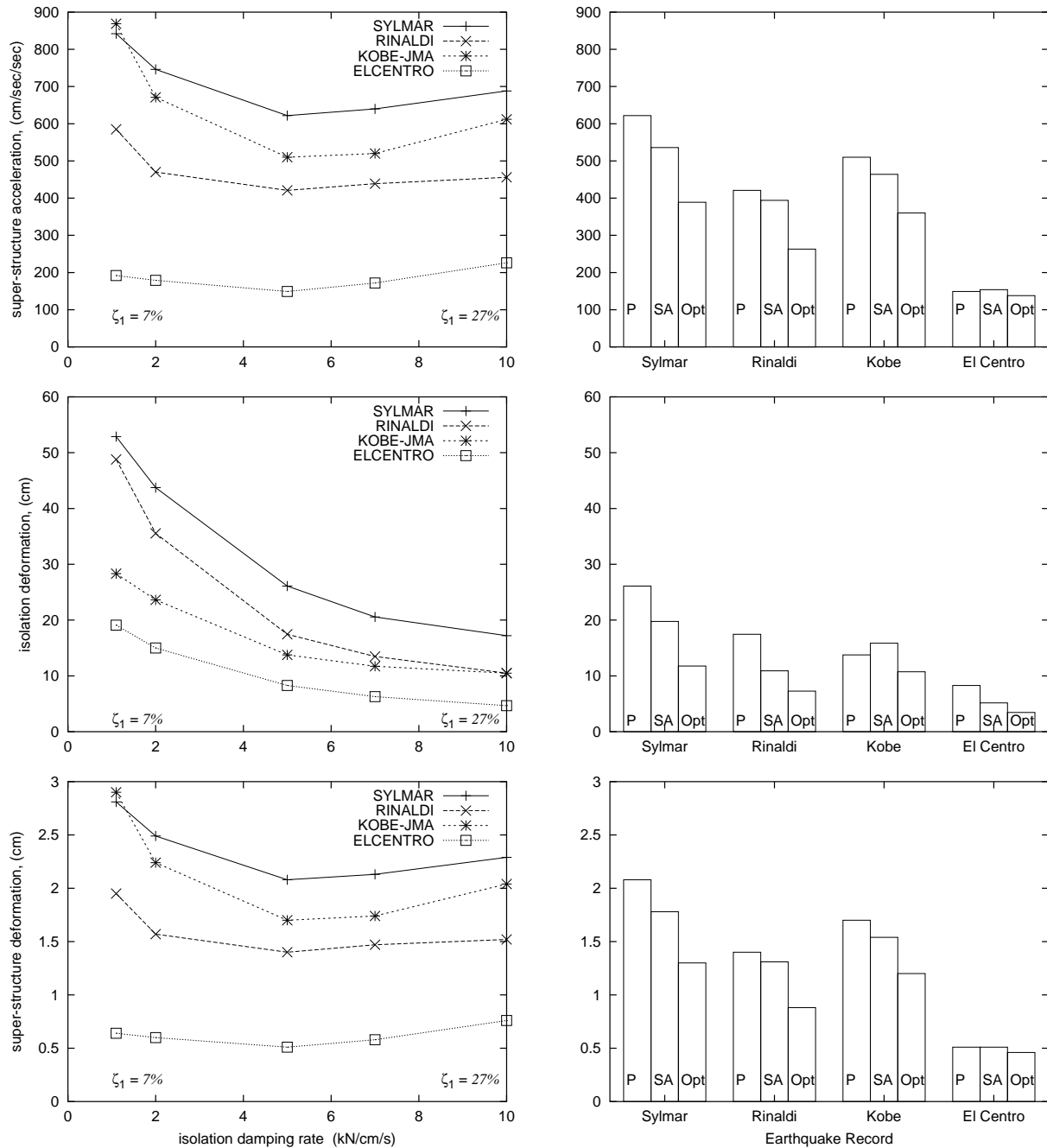


Figure 2: Response of auto-adaptive seismic isolation systems to earthquake excitation. P:passive, SA:semi-active (equation (3)), Opt: optimal semi-active.

Conclusions

In a two-part analysis this study evaluated the *behavior* of auto-adaptive seismic isolation systems and the *response* of auto-adaptive seismic isolation systems to four major earthquakes. Non-linearities in dynamic systems with controllable damping and stiffness prevents

the analytical formation of frequency response functions, however the homogeneity of these systems does allow for computed frequency response functions to be compared. Frequency response functions of several auto-adaptive isolation systems illustrates that a simple feedback control rule can overcome the amplification of accelerations and inter-story drifts caused by large levels of passive viscous damping. The earthquake *response* studies illustrate that auto-adaptive control can reduce the super-structure acceleration and the super-structure deformation below any value achievable via passive viscous damping. Furthermore, this is achieved with isolation deformations that are comparable to very high levels of passive damping.

Acknowledgements

The authors gratefully acknowledge support from the National Science Foundation for this work under award number CMS-9900193, the Scientific Technical Research Council of Turkey (NATO-B1 Research Scholarship) and Istanbul Technical University. The authors are especially grateful to Dr. H. Fujitani of the Building Research Institute (BRI), Tsukuba, Japan, and Dr. C. Minowa of the National Research Institute for Earth Science and Disaster Prevention (NIED), Tsukuba Japan, for valuable discussions and input regarding the development of auto-adaptive seismic isolation systems.

References

1. Dyke, S.J., Spencer, B.F., Sain M.K. and Carlson, J.D. (1996) "Modeling and control of magnetorheological dampers for seismic response reduction." *Smart Mater. and Struct.* vol 5, pp 565–575.
2. Gavin, Henri P. and Dobossy, Mark, "Optimal Design of an MR Device," *Proc. SPIE, 8th Annual International Symposium on Smart Structures and Materials*, 3 – 8 March 2001, Newport Beach, CA.
3. Heaton, T.H., Hall, J.F., Wald, D.J., Halling, M.W., (1995), "Response of high-rise and base-isolated buildings to a hypothetical M_w 7.0 blind trust earthquake," *Science*, 267:206-211.
4. Kelly, J.M., (1999), "The role of damping in seismic isolation," *Earthquake Engineering and Structural Dynamics*, 28:3-20.
5. Kelly, J. M., (1997), *Earthquake-Resistant Design With Rubber*, 2nd edition, Springer Verlag.
6. Lee, Peter L, Mazeika, Aaron, Xu, Joseph, and Mokha, Anoop, (2001) "High-Tech Isolation," *Civil Engineering*, May 2001, p 66-71.
7. EERC, UC Berkeley, (2001), "Seismically-Isolated Buildings in the United States," <http://nisee.berkeley.edu/prosys/usbltdgs.html>

8. EERI SPECIAL EARTHQUAKE REPORT - December 1999 The Chi-Chi, Taiwan Earthquake of September 21, 1999
<http://www.eeri.org/Reconn/Taiwan1299/TaiwanFinal.html>
9. Karnopp, D., Crosby, M.J., and Harwood, R.A., (1974), "Vibration control using semi-active force generators," *ASME Journal of Engineering for Industry*, 96(2): 619-626.
10. Naeim, F. and J.M., Kelly, (1999), *Design of Seismic Isolated Structures : From Theory to Practice*, John Wiley and Sons.
11. Nagarajaiah, S. and S. Xiahong, (2000), "Response of base-isolated USC Hospital Building in Northridge Earthquake," *Journal of Structural Engineering*, 126(10):1177-1186.
12. Sherin, Brian, and Bartoletti, Stacy (1999) Taiwan's 921 Quake: Effects on the Semiconductor Industry and Recommendations for Preparing for Future Earthquakes. EROM Technical Report, EROM, Sunnyvale, CA.
<http://www.semi.org/web/winitatives.nsf/>
13. Skinner, R.I., Robinson, W.H., McVerry, G.H., (1993), *An introduction to seismic isolation*, John Wiley and Sons.
14. Stengel, R.F. (1994) *Optimal Control and Estimation*, Dover Press.